How carbon coating or continuous carbon pitch matrix influence the silicon electrode/electrolyte interface sand the performance in Li-ion batteries

Aude Roland, Julien Fullenwarth, Jean-Bernard Ledeuil, Hervé Martinez, Nicolas Louvain, L. Monconduit

Received: 10 September 2021 | Revised: 10 November 2021 | Accepted: 25 November 2021

DOI: 10.1002/bte2.20210009

RESEARCH ARTICLE

BATTERY ENERGY Open Access WILEY

How carbon coating or continuous carbon pitch matrix influence the silicon electrode/electrolyte interfaces and the performance in Li-ion batteries

Aude Roland[1] | **Julien Fullenwarth**[1] | **Jean-Bernard Ledeuil**[2] | **Hervé Martinez**[2,3] | **Nicolas Louvain**[1,3] | **Laure Monconduit**[1,3]

[1]ICGM, Univ. Montpellier, CNRS, ENSCM, Montpellier, France

[2]Université de Pau et des Pays de l'Adour, IPREM, CNRS UMR 5254, Pau, France

[3]Réseau sur le Stockage Electrochimique de l'Energie (RS2E), FR CNRS 3459, Hub de l'Energie, Amiens, France

Correspondence
Laure Monconduit, ICGM, Univ. Montpellier, CNRS, ENSCM, Montpellier 34293, France.
Email: laure.monconduit@umontpellier.fr

Abstract

The Si surface coating by carbon is an appealing strategy to improve both the electronic conductivity and to stabilize the solid electrolyte interphase (SEI). In the present study, the electrochemical performance comparison of three nanocrystalline silicon-based electrodes confirms the advantage brought by the carbon presence either as coating or in a composite, to improve their performance in Li-ion batteries (LIBs). To rationalize this behavior, a full study of the electrode/electrolyte interface was achieved through the analysis of the cumulated relative irreversible capacity and the impedance and X-ray photoelectron spectroscopies measurements. The study highlighted that the carbon coating leads to more efficient and less resistive SEI than that formed on silicon or on the native oxide surface. The pitch carbon matrix offers the same advantages and avoids moreover the isolation of particles. The control of the Si/electrolyte interface has a crucial role in the performance of Si-based electrodes as negative electrodes for LIB.

KEYWORDS

batteries, negative electrodes, silicon

1 | INTRODUCTION

Silicon is known as one of the best negative electrode candidates for Li-ion batteries (LIBs) applications. Its alloying with lithium may theoretically lead to specific capacities in LIB as high as 3580 mA h g^{-1} with the formation of $Li_{15}Si_4$, the most lithiated phase electrochemically formed at room temperature. The relatively low potential (0.4 V vs. Li^+/Li) of reaction of Si with Li leads to high full cell voltage with a positive electrode such as $LiCoO_2$ with safe cycling conditions in comparison with graphite (0.05 V vs. Li^+/Li). Moreover, Si is abundant on earth, relatively cheap, and also nontoxic. On the cons side, silicon possesses however a high electronic resistivity (10^3 Ω cm) and a low Li^+ diffusion coefficient (D_{Li}+: 1.10^{-14} to 1.10^{-12} $cm^2.s^{-1}$)[1,2] which limits its performance at high current density. Its alloying/dealloying mechanism with Li induces a large volume change that can lead to electrode delamination[3] and rapid capacity fade in cycling.[4,5] Finally, one of the most important concerns for Si-based electrodes is the low coulombic efficiency due to the electrolyte decomposition which occurs continuously on the fresh Si surfaces formed by the cracks of the electrode.[6,7] The solid electrolyte interphase (SEI) formation

from the electrolyte degradation and its evolution in cycling is still the object of intense research in the batteries field. A general consensus is that SEI composition depends on the electrolyte's chemical nature but also on the electrode composition.[8] Most of the common organic electrolyte solvents are reduced at the electrode's surface at low potentials.[9] The SEI was first described as being organized in mosaic. More recently it was described as an inorganic and dense layer in contact with the electrode which is recovered with another organic or polymeric Li^+ conducting layer in contact with electrolyte.[10,11]

To limit the dramatic consequences of the volume expansion, a plethora of solutions have been described in the literature. It is possible to limit the potential window (>50 mV[12]) or the lithiation duration to prevent the crystallized $Li_{15}Si_4$ formation which favors particles pulverization.[13–16] Another strategy consists of nanosizing and nanostructuring the silicon, which reduces the mechanical stress and so the pulverization of the electrode.[17] Nevertheless, this strategy increases the surface area in contact with the electrolyte and amplifies the electrolyte degradation, responsible for a very low coulombic efficiency and a limited cyclability. Therefore interest has grown to protect and stabilize the electrode surface to modify the interface with electrolytes. A strategy consists in adding additives in electrolytes as the fluoroethylene carbonate (FEC) to form a dense, homogeneous, thin, and stable SEI, which remarkably improves the Si-based electrode performance.[18–21]

Another strategy is to modify the Si surface by carbon coating which enhances electronic conductivity. It was also suggested that the carbon coating stabilizes the SEI and enhanced the electrode electronic conductivity.[22] Different carbon sources were tested as pitch,[23–27] acetylene,[28] citric acid,[29] pVdF,[30] glucose,[31] or dopamine,[32] with different deposition methods as PVD, pyrolysis, sol-gel, or hydrothermal.[33] Graphene layers have also been studied and showed encouraging results thanks to their high thermal and chemical stability, their high flexibility, and good electronic conductivity.[34] A thick coating (2–10 nm) demonstrated better capacity retention than a thinner layer (2 nm). Impedance spectrometry measurements (EIS) achieved during lithiation showed that the presence of the thick carbon coating results in a more stable SEI, less resistive leading to improved cyclability.[35] If many strategies to cover the Si surface exist, it is worth noting that the analysis of the impact of this carbon coating especially on the SEI chemical composition is poorly reported in the literature.

The objective of the present study is to evaluate for a nanometric silicon-based electrode the effect of the presence of carbon either as coating of silicon or in a composite on both the SEI nature and its evolution in cycling. Three active materials, Si nanoparticles, carbon-coated silicon nanoparticles, and carbon-coated Si embedded in a carbon matrix were compared. After a deep characterization of these Si samples, especially their surface by XRD, IR-ATR spectroscopy, and SEM, they were tested in lithium batteries. To rationalize both the different performance and aging processes observed for these three electrodes, a full X-ray photoelectron spectroscopies analysis was used to follow the chemical nature and thickness of the SEI. Impedance measurements allowed following the resistance of the three batteries during the cycling.

2 | EXPERIMENTAL SECTION

2.1 | Physico-chemical characterization method

The different active materials have been characterized by Attenuated Total Reflectance Fourier Transform Infrared spectroscopy (ATR-FTIR) using a Spectrum 2 (PerkinElmer; 32 scans – Resolution 4 cm^{-1}) and by X-ray diffraction (XRD) using a Phillips PANalytical X'Pert Pro equipped by a detector X'Celerator and a copper source (Kα1 radiation [$\lambda = 1.5405929$ Å]). Energy Dispersive X-Ray Analysis (EDX) mapping was done using a Zeiss Evo HD15 equipped with an SDD EDX Oxford Instruments X-MaxN detector of 50 mm^2 surfaces.

The X-ray photoelectron spectroscopies measurements were carried out at different states of charge. Each battery was opened in the glove box, the electrode was rinsed three times in 1 ml of DMC. The spectra were recorded with a Kalpha Thermo Electron X-ray photoelectron spectroscopies Spectrometer equipped with a monochromatic Al Kα (1486.6 eV). The analyzed surface was around 400 μm in diameter. Each sample has been probed three times for data reproducibility. Spectra are mathematically fitted with Casa X-ray photoelectron spectroscopies software using a least-squares algorithm and a nonlinear baseline (Shirley). The fitting peaks of the experimental curves are defined by a combination of Gaussian (70%) and Lorentzian (30%) distributions. The quantification is performed using Thermo Fisher Scientific relative sensitivity factors based on the Scofield Cross-sections and all the spectra were calibrated with CC-CH bonding energy at 285 eV.

2.2 | Si-based electrodes elaboration method

Si-based electrodes were elaborated from a slurry prepared by grinding the active material, nanosized Si,

coated nanosized Si (Si@C; furnished by Nanomakers) or the composite formed with Si and pitch (Si@C_250M), with two carbon additives: Super P (H30253 Carbon black Alpha Aesar) and VGCF (VGCF-H, BET = 15 m^2/g, Showa Denko) in an agate mortar and then in a planetary ball-miller (Fritsch sprayer, for 10 min at 500 rpm to maximize the dispersion). Then, the solvent (distilled H_2O) and the carboxymethyl cellulose binder (MW = 250,000; DS = 0.9, Sigma-Aldrich) were added and mixed for 1 h. The slurry was tape cast on a copper current collector (Goodfellow copper foil: 99.9% Cu, 0.0175 mm thick) at a 150 nm thickness (3540, Elcometer). The electrode film was dried for 24 h at room temperature (away from drafts), cut at a 12.7 mm diameter, and dried under vacuum at 80°C in a Büchi overnight. The electrodes were stored in a glove box before the electrochemical test. The Si and Si@C-based electrodes were elaborated with the ratio (active material [AM]/[SuperP/VGCF] [50/50]/CMC) of (18/70/12) wt% respectively. The Si@C_250M composite-based electrode was elaborated with a ratio Si@C_250M/SuperP-VGCF/CMC of 80/5/15 (taking into account that the composite Si@C_250M contains 12 wt% of Si, previously estimated[27]).

The total material loading for all samples was approximately 1.2 mg cm^{-2} (0.25 mg/cm^2 for Si), corresponding to a density of 0.4 g cm^{-3} approximately.

2.3 | Coin cell elaboration method

Coin cells (2032) were assembled in an Argon-filled glovebox and used for the evaluation of electrochemical cycling performance. The coin cell was composed of the Si-based working electrode and a lithium foil at the counter electrode, the two electrodes were separated by a glass-fiber paper (GF/D, Whatman) soaked with the electrolyte. The electrolyte used was Lithium hexafluorophosphate ($LiPF_6$) 1 M in Ethylene Carbonate: Propylene Carbonate: 3 Dimethyl Carbonate (EC/PC/3DMC) (Solvionic), 5%v of Fluoro Ethylene Carbonate FEC (98% purity, Alfa Aesar), and 1%v Vinylene Carbonate (VC) (80 ppm BHT as a stabilizer, 99% purity) were added.

2.4 | Electrochemical tests

Galvanostatic experiments were conducted using a BCS-805 Battery cycling system (10 V, 150 mA) from BioLogic Science Instruments using CR2032-type coin cells between 1.5 and 0.01 V at room temperature. For the first cycle, a current density of C/20 (178 mA g^{-1}) was applied to activate the electrode then the current density was increased at C/5 (716 mA g^{-1}) during 100 cycles.

For the calculation of specific capacity, the weight of both carbons (Super P, carbon fibers) and silicon particles were considered. For Si and Si@C-based electrodes, the expected specific capacity is then 775 mA h $g^{-1}_{(Si+C)}$. By considering the experimental capacity value of the pitch (185 mA h g^{-1}) and the theoretical capacity of silicon (3580 mA h g^{-1}), and taking into account a Si content of 12 wt% in the composite, previously estimated,[27] the Si@C_250M based electrode is expected to have a theoretical capacity of 640 mA h g^{-1}.

Electrochemical impedance spectroscopy measurements were carried out using a potentiostat (from BioLogic Science Instruments) using Swagelok three-electrode setting with a Li foil at the counter and reference electrode. The measurements for Si and Si@C-based electrodes were realized with a Si/C/CMC ratio of 70/18/12 to maximize the active material/electrolyte interface effect on the impedance observed. As in these conditions, high performances are not aimed at, the impedance study was realized only on the first cycle. Electrochemical impedance spectroscopy measurements were recorded after 30 min OCV, after a first discharge at a current rate of C (I = 3600 mA h g^{-1}(Si)) and after 1 h rest to stabilize the potential and after one charge and 1 h of stabilization.

3 | RESULTS AND DISCUSSION

3.1 | Physicochemical characterization results

Crystalline silicon nanoparticles supplied by Nanomakers are produced at an industrial scale by laser pyrolysis method from silane precursor. Silicon particles with a thin carbon coating (Si@C) were elaborated using a double-stage process from carbonaceous precursors.[36] Si-pitch composite named SiC_250M was prepared using the method described in an earlier publication.[27] It was shown that Si is fully embedded in a continuous carbon matrix (see Supporting Information SI1).

Previous nitrogen adsorption measurements showed that the average silicon particles size is around 78 nm diameter for Si and 80 nm for silicon with carbon coating Si@C.[27] XRD measurements for the three samples (Figure 1) indicate a cubic structure (ICSD 00-026-1481, *Fd*-3*m* space group). No additional peak was observed from silicon oxide or from the carbon coating. Thus, the carbon coating and the composite preparation do not modify the Si crystallographic structure.

ATR-FTIR analyses (Figure 2) show the chemical groups present at the Si surface, with the characteristic bands from Si-O-Si bonds between 1750 and 400 cm^{-1}. Si-OH bands are

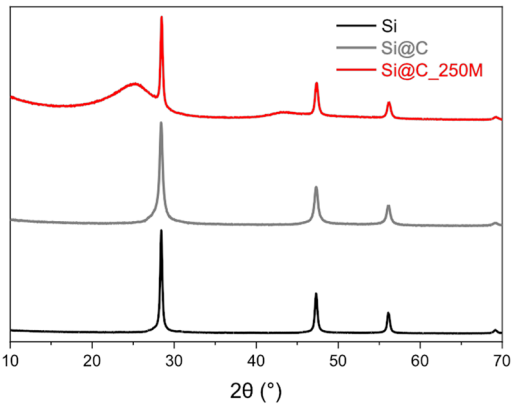

FIGURE 1 X-ray diffraction powder pattern of Si, Si@C, and Si@C_250M samples

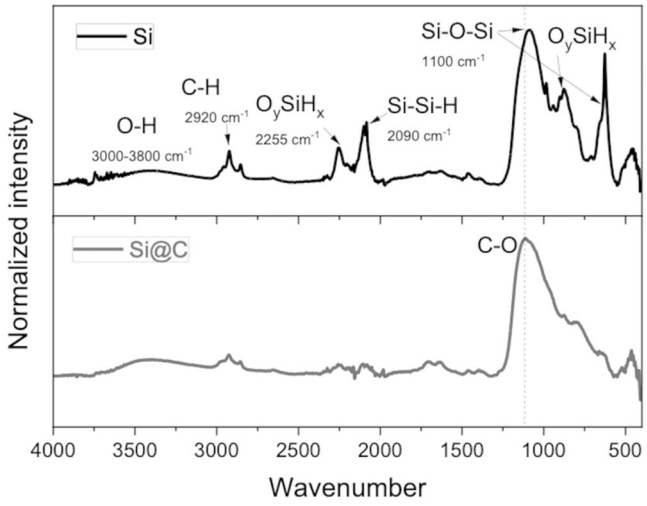

FIGURE 2 ATR-FTIR spectra of Si and Si@C powders

observed between 3000 and 3500 cm^{-1} and Si-H bands between 2000 and 2150 cm^{-1},[37,38] which indicate a partial Si surface oxidation, certainly the native SiO_2 layer. All the carbon-coated silicon bands present a lower intensity and one dominates around 1550 cm^{-1} probably attributable to C-O vibration from the carbon coating.[37,38] As carbon is a well-known reducing media, it is likely able to modify the SiO_2 layer into Si or SiO_x layer (with $x < 2$).

The SEM-EDX mapping of the electrodes prepared from the three samples (Figure 3) shows at this micrometric scale a homogenous Si repartition in all cases. The Si@C_250M electrode shows a more porous structure with more visible dark pores.

3.2 | Electrochemical characterization

The first cycle galvanostatic curves (Figure 4; normalized to clarify the comparison) show very close behavior for the Si and Si@C lithiation with the same shape of discharge and charge and a close coulombic efficiency (CE1). The first discharge shows a quick potential drop until 0.01 V and then a potential plateau ascribed to the crystalline Si lithiation into amorphous Li_xSi.[39] In charge, after a progressive increase of potential with Li deinsertion, a small plateau is observed around 0.46 V versus Li^+/Li which is typical of the $Li_{15}Si_4$ delithiation.[39] For Si@C_250M, the potential drops rapidly from the OCV until 0.7 V versus Li^+/Li. Then, unlike the two previous samples, the potential decreases slower until 0.06 V and the plateau at 0.01 V is shorter. Between 0.7 and 0.1 V, the region can correspond to the Li reaction with the pitch in good agreement with the galvanostatic curve collected for pitch alone.[27] For Si, Si@C, and Si@C_250M, the first discharge capacities, 1024, 973, and 805 mA h g^{-1}, are systematically higher than the expected theoretical ones 775, 775, and 640 mA h g^{-1} according to their formulation. It is attributable to the contribution of the SEI. The coulombic efficiency (CE1) is slightly lower for the composite Si@C_250M (76.9%) than for Si (78.8%), and Si@C (80%; Table 1) which confirms that the SEI contribution is likely more important in the first cycle for the Si-pitch composite. It is worth noticing that the CE reaches more rapidly its maximum in cycling with the pitch composite than with other Si samples. Moreover, after 100 cycles the capacity faded more rapidly for Si and Si@C than for Si@C_250M, with a retention of 69%, 78%, and 95% of the first cycle reversible capacity, respectively. Both carbon coating and pitch clearly show their advantages for cycling performance.

To better understand the reason of the aging of the Si electrodes the relative irreversible capacity (RIC) was calculated with the following equation. It allows separating the capacity loss coming from the particles' disconnection from that coming from the SEI formation[40]:

$$RIC_{disconnection} = \frac{C_{Cn} - C_{Cn+1}}{C_{Cn}}$$

$$RIC_{SEI} = \frac{C_{Dn} - C_{Cn+1}}{C_{Cn}}$$

with C_{Cn} and C_{Cn+1} corresponding to the charge capacity at the n and n+1 cycle and C_{Dn} the discharge at n discharge.

The capacity difference in charge between n and n+1 represents the capacity loss due to the particles' disconnections and the difference between the discharge at cycle n and the charge at cycle n+1 corresponds to the capacity loss due to the SEI formation. One can observe with the cumulated RIC (Figure 5) that the continuous SEI formation contributes mainly to the capacity fade in

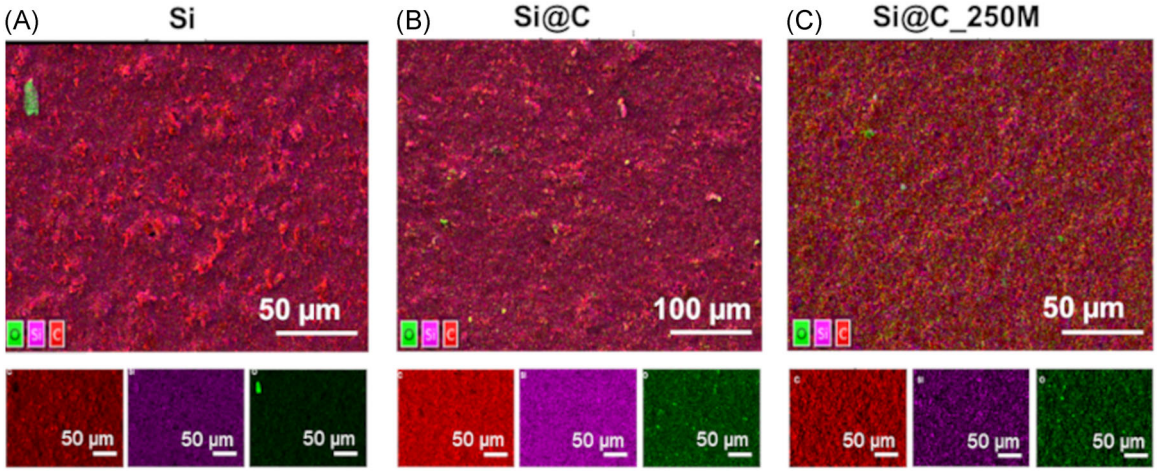

FIGURE 3 SEM-EDX mapping of Si-based (A), Si@C-based (B), and Si@C_250M-based electrodes (C)

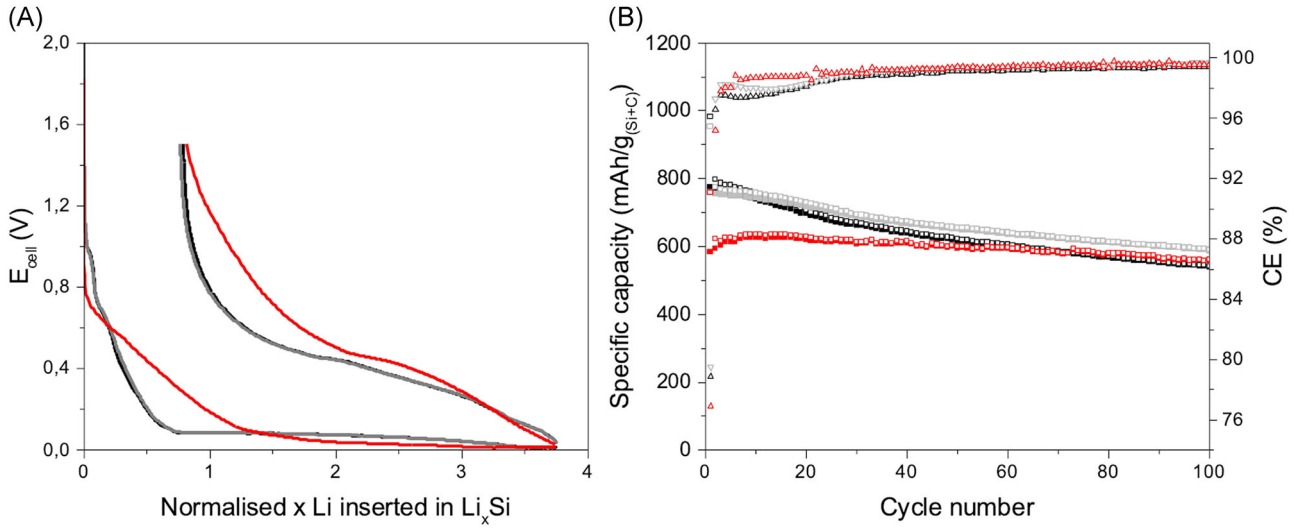

FIGURE 4 (A) First galvanostatic cycle normalized curves obtained by applying a current of 400 mA $g^{-1}_{(Si+C)}$; (B) The capacity (left) retention and the coulombic efficiency (right) as a function of cycle number, obtained at 1500 mA.$g^{-1}_{(Si+C)}$, for Si (black), Si@C (gray), and Si@C_250 M (red)

TABLE 1 Table of cycling performance (averaged values from three batteries)

Active material	Capacity 1st discharge (mA h g^{-1})	Capacity 1st charge (C1) (mA h g^{-1})	Coulombic efficiency 1st cycle (CE1)	Coulombic efficiency 10st cycle (CE10)	Capacity 100st charge (C100) (mA h g^{-1})	Coulombic efficiency 100st cycle	C100/C1
Si	1024	775	78.8	97.5	539	99.4	0.69
Si@C	973	759	80.0	98.0	589	99.7	0.78
Si@C250M	805	583	76.9	98.7	553	99.4	0.95

Abbreviations: C, capacity; C, charge; CE, coulombic efficiency; D, discharge; n, number of cycle.

these three Si electrodes, however, a different evolution can be noticed. First, Si@C_250M shows a more rapid capacity loss for the first 10 cycles than the two other samples. Then, up to 100 cycles, the Si electrode accumulates more rapidly the capacity loss due to the SEI formation than the carbonaceous Si electrodes Si@C and Si@C_250M. Lower losses due to the disconnection are observed for the Si@C_250M electrode and can be attributable to enhanced electronic percolation of the carbon matrix. A different SEI in terms of chemical species or

morphology for the Si@C_250M could explain such differences and are investigated in the next part.

The positive effect of this carbon coating is therefore verified by galvanostatic measurements (Figure 4) over 100 cycles and is probably due to the formation of an SEI more stable on the carbonaceous surface than on the surface of silicon or native oxide. Although not stretchable, this carbon coating seems not to alter the connectivity between the Si particles and the CMC binder since the capacity loss is lower than with the Si particles without the C coating. A deeper analysis will be required to understand how Si-CMC covalent bonds can be maintained in presence of the carbon coating.

To better understand the difference in the SEI (nature, thickness, or resistivity), electrochemical impedance spectroscopy and post-mortem X-ray photoelectron spectroscopies measurements were performed on the three Si electrodes. The Nyquist plot (Figure 6) shows the impedance evolution during the first cycle. Si@C_250M electrode presents a higher resistance than the Si and Si@C electrodes during the OCV, certainly due to the lower conductivity of Pitch compared to Super P and VGCF, these latter being in much higher amount in the Si, Si@C samples. After OCV, close impedance values were observed for Si and Si@C electrodes. After the first lithiation (discharge), a significant reduction in these impedances is observed for all samples. The decrease in impedance observed at the end of discharge can be explained by a higher electronic conductivity of the lithiated phases Li_xSi, as well as by the increase of the volume of Li_xSi, which raises the pressure on the percolating network and improves the electrical contacts with the current collector. At the end of the charge, the resistances changed only slightly. The electrode impedance of Si@C_250M sample in OCV is very high, much higher than those of Si and Si@C and decreases sharply at the end of discharge. At the end of the charge, the impedance is higher than that of the other two systems but in the same magnitude order of the two others.

Electrochemical impedance spectroscopy measurements show an impedance improvement for Si@C sample compared to Si but would be completed for further cycling to explain the best cycling behavior observed for Si@C_250M. This seems to be in good agreement with the cumulated RIC which indicates that the most important improvement of Si@C_250M lies in the current collector contact. An equivalent electrical circuit model (please refer to Figure SI6) is proposed to extract the values of the electrical components attributable to physical phenomena taking place during the electrochemical processes involved in the battery.

From the fit, the resistance resulting from the SEI increases at the end of the lithiation of the material,

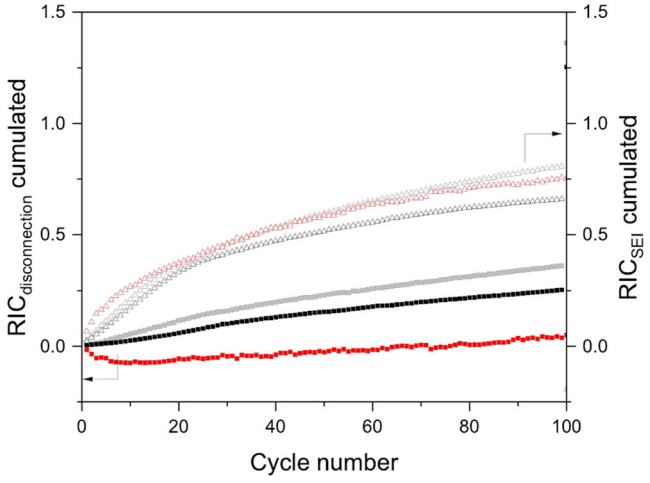

FIGURE 5 Cumulated relative irreversible capacity due to the Solid Electrolyte Interphase formation and the disconnection of particles from the current collector for the Si, Si@C, and Si-250M electrodes (for Si [grey], Si@C [black], and Si@C_250M [red])

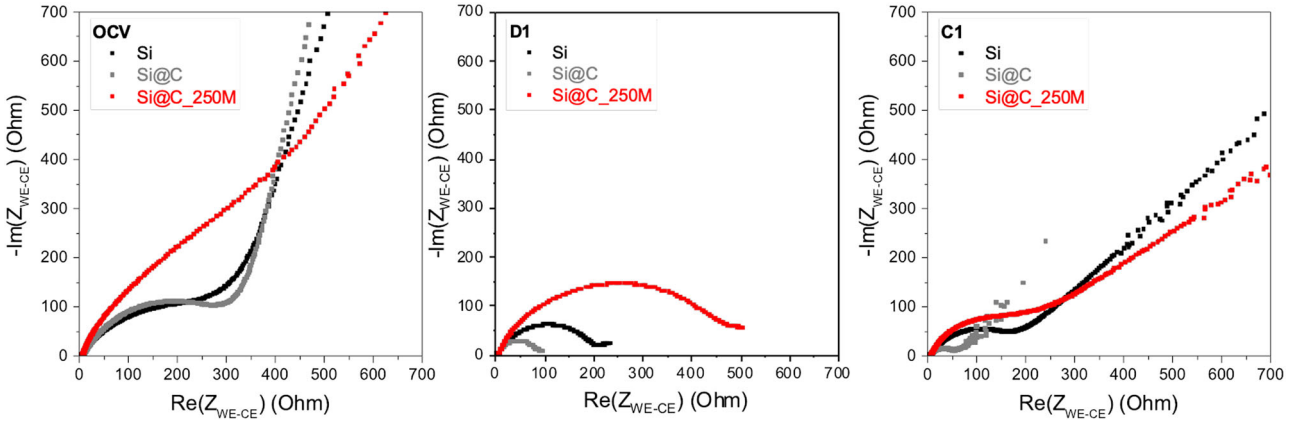

FIGURE 6 Nyquist plot of electrochemical impedance spectroscopy realized after 30 min of OCV, end of the first discharge (D1), and the end of the first charge (C1) for Si, Si@C, and Si@C_250M

as expected from the electrolyte instability at low potential.[35] The SEI resistance decreases slightly in charge, probably due to a slight dissolution of the SEI layer.[41] The SEI resistance values are three times lower for Si@C than for Si in good agreement with the cumulated RIC evolution (Figure 6). The carbon coating induces a less resistive SEI formation which is in good agreement with other studies. To understand the various behaviors of the three Si-based electrodes, the SEI was studied for the X-ray photoelectron spectroscopies analysis before (Figure 7) and after cycling (Figure 8).

3.3 | Comparison of the three-electrode surfaces before cycling

The high-resolution X-ray photoelectron spectroscopies spectra (C 1s, O 1S, and Si 2p) of the components of the electrodes, the conductor additives (Super P and VGCF), and the binder (CMC) were identified from references and presented in detail in SI 4. From these identifications, the different components of the Si, Si@C, and Si@C_250M pristine electrodes were identified, quantified and reported in Figure 7. Very similar species distribution is observed for the Si and Si@C pristine electrodes with approximately 1/3 of the surface composed of Si, 1/3 of carbon additives, and 1/3 of contamination species and CMC binder. However, silicon oxide is less present in Si@C, indicating that the carbon coating limits the oxidation of the silicon during the storage and/or preparation of the electrode. For the pitch-based electrode Si@C_250M, the silicon and its oxide are very visible, they represent half of the species on the surface of the electrode, which could indicate an inhomogeneity of the pitch and silicon dispersion despite its apparent homogeneity measured at micro-metric scale by EDX mapping. We also observe a greater ratio of oxidized carbon (C-O type) coming likely from the pitch.

3.4 | Comparison of the three electrode surfaces during cycling

3.4.1 | Thickness of the solid electrolyte interphase

From the analysis of the different spectra collected during cycling after discharge and charge for the 1st and the

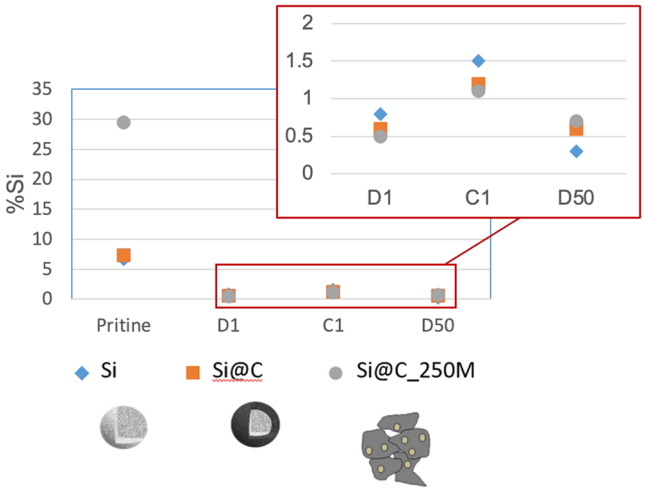

FIGURE 8 Evolution of the Si ratio as a function of the state of charge of the Si (in blue), Si@C (in orange), and Si@C_250M electrodes (in gray)

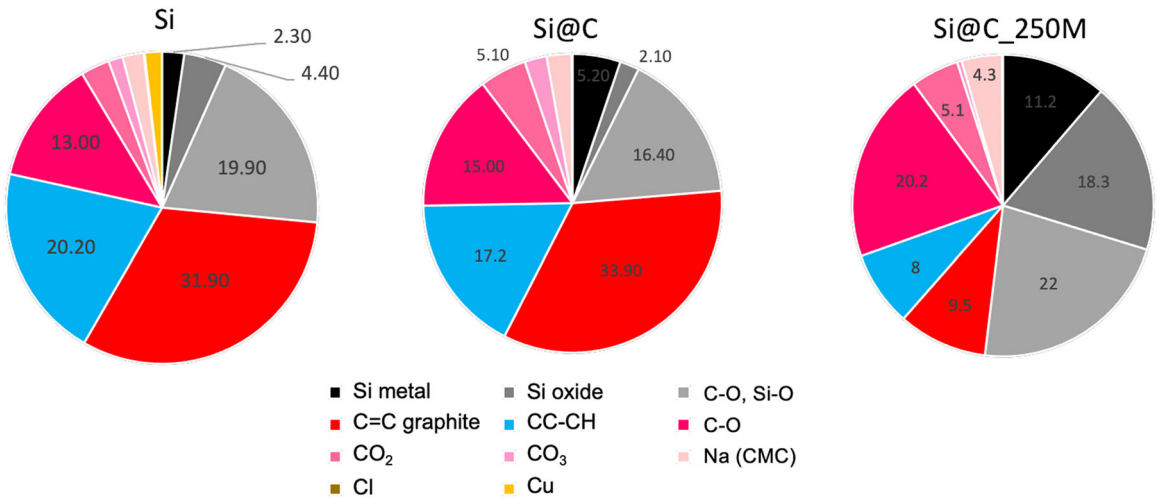

FIGURE 7 X-ray photoelectron spectroscopies chemical analysis of the Si, Si@C, and Si@C_250M pristine electrodes

50th cycles, and for the three electrodes, it is possible to extract the Si ratio (Figure 8).

After a first discharge, for all samples, the amount of Si decreases drastically due to the recovering of the surface by a thick SEI layer. Although Si is more present in Si@C_250M pristine electrode surface than for Si@C and Si ones, after the first discharge, the reverse trend is observed, indicating that a thicker SEI layer formed at the Si-based electrode surface. After the charge for all samples, the Si ratio increases again indicating a partial dissolution of the SEI during the charge. As the X-ray photoelectron spectroscopies probe, the first 5–10 nm of the sample and that approximately 95% of the signal comes from the last 5 nm, we can deduce that the thickness of the SEI remains less than 10 nm in the first cycle. A complementary study by transmission electronic microscopy (TEM) analysis should be considered to assume that the SEI layer is uniform and confirm the conclusions about its layer.

3.4.2 | Electrodes surface after 50 cycles

The full analysis of the surface by X-ray photoelectron spectroscopies (spectra of the C1s, Si 2p, O1s, and F1s core peaks) was performed for the three samples and is presented in Supplementary Informations SI4, SI5, and SI6 for the Si sample for pristine electrode, after OCV, after the first discharge (D1) and charge (C1) and after 50 cycles (D50 and C50) to follow the evolution of the SEI.

The Si(0) peak disappears on discharge (D50) and appears clearly after the charge (C50), suggesting that the formation/dissolution phenomenon of the SEI is still preponderant. On the other hand, the graphite peaks initially around 284 eV for carbon additives have completely disappeared (Figure SI5), suggesting the SEI is thicker on the carbon particles or a migration of Si particles to the surface induced by material pulverization. Similar compositions and the same cycling SEI behavior were observed for the Si@C and Si@C_250M electrodes (Figure SI6). The main components of the SEI identified for the three electrodes are LiF, Li_2CO_3, and Li_2O. Their quantifications were obtained from fit (Supplementary Information SI6) and are summarized in Figure 9.

After OCV, it is observed that the LiF species, arising from the salt degradation, are preponderant for the Si and Si@C_250M electrodes and that the formation of Li_2CO_3 is more important in the case of Si@C. At the end of the first discharge Li_2CO_3 increases widely for all samples, it is the majority species. The amount of Li_2CO_3 is higher in the electrodes with carbon, Si@C, and Si@C_250M. A significant proportion of Li_2O is detected for electrode Si, and less for the electrodes Si@C and

FIGURE 9 Electrode surface composition evolution while cycling

Si@C_250M. At the end of the first charge, the ratio of Li_2CO_3 is reduced, likely dissolved in the electrolyte. Simultaneously LiF ratio increased for all the samples, and more for the carbon samples. It can be suggested that the dissolution of the carbonates unearths the buried LiF. After 50 cycles, there is still a significant formation of Li_2CO_3 in discharge, which continues to be dissolved in charge for the three samples, especially for the Si electrode. A large accumulation of Li_2O takes place for the Si electrode, a result that may be linked to lower electrochemical performance for this compound.

In conclusion, X-ray photoelectron spectroscopies surface analysis reveals a clear difference of the SEI between the Si electrodes and the Si-carbon electrodes, in terms of

thickness as well as of evolution in cycling. The presence of carbon, either as coating or as the matrix, seems to guarantee a thinner SEI layer which is richer in carbonates and poorer in Li_2O and LiF than in the case of Si alone.

4 | CONCLUSION

We compared the electrochemical performance of the silicon-based electrodes Si, Si@C, and Si@C_250M. The carbon coating is advantageous for the performance of nanosized silicon electrodes, with in particular the maintenance of 78% of the capacity after 100 cycles for Si@C versus 69% for Si without carbon coating. The pitch matrix allows still increasing the performance with the maintenance of 95% of capacity after 100 cycles. The coulombic efficiency of the Si@C_250M reached rapidly the value of 99.5% as for Si and Si@C samples it increased progressively to stabilize after 20 cycles around 99.5%. This different SEI formation was clearly highlighted by the cumulated RIC analysis that showed the presence of carbon as coating or matrix decreases the capacity fading due to the SEI formation. A full Electrochemical impedance spectroscopy study should be planned to get deeper information on the evolution of the resistance of the cell, however, preliminary measurements show a clear decrease of resistance after one cycle, especially for carbon-coated Si sample.

X-ray photoelectron spectroscopies were a powerful tool to identify the reason for the better behavior of Si with carbon coating or in a pitch matrix. X-ray photoelectron spectroscopies demonstrated that the presence of carbon in the Si electrode does not modify the nature of the species of the SEI layer, however, influences their ratio, in the pristine (in OCV) as well as in cycled electrode. Although the SEI layers are continuously accumulating for Si, this is less the case for Si-carbon electrodes with likely more species dissolution in the electrolyte in successive charges. These observations are in good agreement with the cumulated RIC analysis.[42]

The presence of carbon (coating or matrix) favors the formation of an SEI rich in Li_2CO_3 along cycles, while for the Si electrode the SEI layer is becoming richer in LiF and Li_2O. Let us remember that Li_2O is usually not favorable for good cycling performance and can partially explain the lower performance of the electrode Si. As a matter of fact, the impedance of the SEI deposited on the carbon coating was measured three times lower than that deposited on the bare silicon. The cumulated RIC analysis suggested that the carbon presence, especially in the case of the composite with pitch, Si@C_250M, limits the capacity loss attributable to the disconnection of particles. To conclude, this study highlights the importance of controlling the Si-electrolyte interface to improve the performance of Si-based electrodes as negative electrodes for LIB. The carbon coating allows forming an efficient and less resistive SEI on the carbonaceous surface than on silicon or native oxide when the carbon matrix offers the same advantages and moreover avoids the isolation of particles.

ACKNOWLEDGMENTS

The SEM measurements were performed by Didier Cot, the EDX measurements by Bertrand Rebiere at IEM (UMR5635). The authors thank the Nanomakers for providing the Si powder. This study has benefited from the grant of the National Agency for Research (ANR) under the program "Investments for future" bearing the references ANR-10-LABX-05-01 and Labex STORE-EX, ANR-10-LABX-76-01.

CONFLICT OF INTERESTS

The authors declare that there are no conflict of interests.

AUTHOR CONTRIBUTIONS

Aude Roland: Electrodes preparation, electrochemical measurements, XRD, SEM. Jean-Bernard Ledeuil: X-ray photoelectron spectroscopies analysis. Hervé Martinez: X-ray photoelectron spectroscopies analysis supervising. Julien Fullenwarth: Electrochemical measurements. Nicolas Louvain: Electrochemical and impedance measurement and analysis. Laure Monconduit: Electrochemical mechanism understanding and supervising of the whole study. The authors strongly encourage authors to include author contributions and recommend using CRediT for standardized contribution descriptions. Please refer to our general author guidelines for more information about authorship.

DATA AVAILABILITY STATEMENT

The data presented in this study are available on request from the corresponding author.

ORCID

Jean-Bernard Ledeuil http://orcid.org/0000-0002-7366-2190
Hervé Martinez http://orcid.org/0000-0002-6621-199X
Nicolas Louvain http://orcid.org/0000-0001-8727-6832
Laure Monconduit http://orcid.org/0000-0003-3698-856X

REFERENCES

1. Ding N, Xu J, Yao YX, et al. Determination of the diffusion coefficient of lithium ions in nano-Si. *Solid State Ionics*. 2009; 180:222-225.
2. Domi Y, Usui H, Shimizu M, Kakimoto Y, Sakaguchi H. Effect of phosphorus-doping on electrochemical performance of silicon negative electrodes in lithium-ion batteries. *ACS Appl Mater Interfaces*. 2016;8:7125-7132.

3. Yuan X, Liu H, Zhang J. Erratum: Borderud SP, Li Y, Burkhalter JE, Sheffer CE and Ostroff JS. Electronic cigarette use among patients with cancer: characteristics of electronic cigarette users and their smoking cessation outcomes. *Cancer. Lithium Ion Batter*. 2007;121:418.
4. Wu H, Cui Y. Association of stroke with the receptor-binding profiles of antipsychotics-a case-crossover study. *Nano Today*. 2012;7:414-421.
5. Zhang WJ. A review of the electrochemical performance of alloy anodes for lithium-ion batteries. *J Power Sources*. 2011;196:13-24.
6. Su X, Wu Q, Li J, et al. Silicon-based nanomaterials for lithium-ion batteries: a review. *Adv Energy Mater*. 2014;4:1300882.
7. Liang B, Liu Y, Xu Y. Silicon-based materials as high capacity anodes for next generation lithium ion batteries. *J Power Sources*. 2014;267:469-490.
8. Eshetu GG, Figgemeier E. Confronting the challenges of next-generation silicon anode-based lithium-ion batteries: role of designer electrolyte additives and polymeric binders. *ChemSusChem*. 2019;12(12):2515-2539.
9. Yaakov D, Gofer Y, Aurbach D, Halalay IC. On the study of electrolyte solutions for Li-ion batteries that can work over a wide temperature range. *J Electrochem Soc*. 2010;157:A1383.
10. Chan CK, Ruffo R, Sae Hong S, Cui Y. Surface chemistry and morphology of the solid electrolyte interphase on silicon nanowire lithium-ion battery anodes. *J Power Sources*. 2009;189:1132-1140.
11. Gauthier M, Carney TJ, Grimaud A, et al. Electrode-electrolyte interface in Li-ion batteries: current understanding and new insights. *J Phys Chem Lett*. 2015;6(22):4653-4672.
12. Ding N, Xu J, Yao Y, Wegner G, Lieberwirth I, Chen C. Improvement of cyclability of Si as anode for Li-ion batteries. *J Power Sources*. 2009;192:644-651.
13. Obrovac MN, Chevrier VL. Alloy negative electrodes for Li-ion batteries. *Chem Rev*. 2014;114:11444-11502.
14. Chevrier VL, Liu L, Le DB, et al. Evaluating Si-based materials for Li-ion batteries in commercially relevant negative electrodes. *J Electrochem Soc*. 2014;161:A783-A791.
15. Iaboni DSM, Obrovac MN. Li 15 Si 4 formation in silicon thin film negative electrodes. *J Electrochem Soc*. 2016;163:A255-A261.
16. Gao H, Xiao L, Plümel I, et al. Parasitic reactions in nanosized silicon anodes for lithium-ion batteries. *Nano Lett*. 2017;17:1512-1519.
17. Feng K, Li M, Liu W, et al. Silicon-Based Anodes for Lithium-Ion Batteries: from Fundamentals to Practical Applications. *Small*. 2018:14.
18. Etacheri V, Haik O, Goffer Y, et al. Effect of fluoroethylene carbonate (FEC) on the performance and surface chemistry of Si-nanowire Li-ion battery anodes. *Langmuir*. 2012;28:965-976.
19. Jung R, Metzger M, Haering D, et al. Consumption of fluoroethylene carbonate (FEC) on Si-C composite electrodes for Li-ion batteries. *J Electrochem Soc*. 2016;163:A1705-A1716.
20. Choi NS, Yew KH, Lee KY, Sung M, Kim H, Kim SS. Effect of fluoroethylene carbonate additive on interfacial properties of silicon thin-film electrode. *J Power Sources*. 2006;161(2):1254-1259.
21. Li Q, Liu X, Han X, et al. Identification of the solid electrolyte interface on the Si/C composite anode with FEC as the additive. *ACS Appl Mater Interfaces*. 2019;11(15):14066-14075.
22. Terranova ML, Orlanducci S, Tamburri E, Guglielmotti V, Rossi M. Si/C hybrid nanostructures for Li-ion anodes: an overview. *J Power Sources*. 2014;246:167-177.
23. Yong Y, Fan LZ. Silicon/carbon nanocomposites used as anode materials for lithium-ion batteries. *Ionics*. 2013;19:1545.
24. Tang F, Lei J, Cui Z, Ouyang J, Liu G, Zhao L. Fabrication, characterization and electrochemical properties of porous coral-structured Si/C composite anode for lithium ion battery. *Trans Nonferrous Met Soc China*. 2015;25:4046-4053.
25. Yang Y, Wang Z, Yan G, et al. Pitch carbon and LiF co-modified Si-based anode material for lithium ion batteries. *Ceram Int*. 2017;43(12):8590-8595.
26. Lee EH, Jeong BO, Jeong SH, Kim TJ, Kim YS, Jung Y. Effect of carbon matrix on electrochemical performance of Si/C composites for use in anodes of lithium secondary batteries. *Bull Korean Chem Soc*. 2013;34:1435-1440.
27. Escamilla-Pérez AM, Roland A, Giraud S, et al. Pitch-based carbon/nano-silicon composite, an efficient anode for Li-ion batteries. *RSC Adv*. 2019;9:10546-10553.
28. Zhang L, Rajagopalan R, Guo H, Hu X, Dou S, Liu H. A Green and Facile way to prepare Granadilla-like silicon-based anode materials for Li-ion batteries. *Adv Funct Mater*. 2016;26:440-446.
29. Gu P, Cai R, Zhou Y, Shao Z. Si/C composite lithium-ion battery anodes synthesized from coarse silicon and citric acid through combined ball milling and thermal pyrolysis. *Electrochim Acta*. 2010;55:3876-3883.
30. Xu Y, Yin G, Ma Y, Zuo P, Cheng X. Nanosized core/shell silicon@carbon anode material for lithium ion batteries with polyvinylidene fluoride as carbon source. *J Mater Chem*. 2010;20:3216.
31. Li W, Tang Y, Kang W, et al. Core-shell Si/C nanospheres embedded in bubble sheet-like carbon film with enhanced performance as lithium ion battery anodes. *Small*. 2015;11:1345-1351.
32. Wang L, Gao B, Peng C, et al. Bamboo leaf derived ultrafine Si nanoparticles and Si/C nanocomposites for high-performance Li-ion battery anodes. *Nanoscale*. 2015;7:13840-13847.
33. Liu P, Zhu K, Gao Y, Luo H, Lu L. Recent progress in the applications of vanadium-based oxides on energy storage: from low-dimensional nanomaterials synthesis to 3D micro/nano-structures and free-standing electrodes fabrication. *Adv Energy Mater*. 2017;7(23):1.
34. Luo J, Zhao X, Wu J, Jang HD, Kung HH, Huang J. Crumpled graphene-encapsulated Si nanoparticles for lithium ion battery anodes. *J Phys Chem Lett*. 2012;3:1824-1829.
35. Bernard P, Alper JP, Haon C, Herlin-Boime N, Chandesris M. Electrochemical analysis of silicon nanoparticle lithiation – effect of crystallinity and carbon coating quantity. *J Power Sources*. 2019;435:226769.
36. Leconte Y, Sublemontier O, Herlin-boime N, Reynaud C, Porterat D. Quinsac. *axelle*. 2013: WO2014079997.
37. Canham L, ed. Handbook of Porous Silicon. 2014:129-134. ISBN: 978-3-319-05743-9.
38. Delpuech N, Mazouzi D, Dupré N, et al. Critical role of silicon nanoparticles surface on lithium cell electrochemical performance analyzed by FTIR, Raman, EELS, XPS, NMR, and BDS spectroscopies. *J Phys Chem C*. 2014;118:17318-17331.
39. MN, Obrovac, L, Christensen. Structural changes in silicon anodes during lithium insertion/extraction. *Electrochem Solid-State Lett*. 2004;7:A93.

40. Gauthier M, Mazouzi D, Reyter D, et al. A low-cost and high performance ball-milled Si-based negative electrode for high-energy Li-ion batteries. *Energy Environ Sci*. 2013;6:2145.
41. Leroy S, Blanchard F, Dedryvère R, et al. Surface film formation on a graphite electrode in Li-ion batteries: AFM and XPS study. *Interface Anal*. 2005;37:773-781.
42. Roland A, Delarre B, Ledeuil J-B, Louvain N, Martinez H, Monconduit L. Silicon-based electrodes formulation in buffered solution for enhanced electrode-electrolyte interfaces. *J Power Sources*. 2021;489:229465.

AUTHOR BIOGRAPHIES

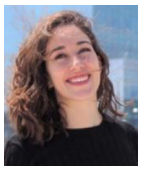

Aude Roland received her PhD degree in chemistry of materials at the University of Montpellier in 2019. Her research is focused on silicon-based negative electrodes for Li-ion batteries and core-shell materials. After a post-doc at the University of Montréal where she worked on concentrated electrolytes, she is currently an R&D engineer at Automotive Cells Company (ACC).

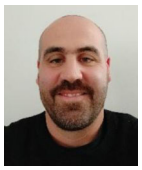

Julien Fullenwarth is Research Engineer at the University of Montpellier, working He is specialist in Surface sciences and material characterization on Li-ion batteries at Institute Charles Gerhardt (ICGM). He is specialist in material characterization by electrochemistry, XRF, XRD.

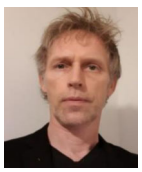

Jean Bernard Ledeuil is Research Engineer at the Université de Pau et des Pays de l'Adour in France in the Department Institut des Sciences Analytiques et de Physico-chimie pour l'Environnement et les Matériaux (IPREM). He is specialist in Surface sciences and material characterization, in Analytical technics (Auger spectroscopy; XPS analysis, Tof SIMS...), with specific preparation technics: ion milling cross section, microtome, polishing... Its field of Applications is energy storage, corrosion study, microelectronics, catalysts, Environment, Health, Polymers.

Hervé Martinez is full Professor in solid-state chemistry at the Université de Pau et des Pays de l'Adour in France. He is at present director of a CNRS Research Federation dedicated to photoemission Spectroscopies and deputy director of UPPA' Faculty of Science and Technology for Energy and Environment (STEE). Its current research fields include the materials surface and interface applied to energy storage (Li(Na)-ion batteries, redox processes and surface phenomena during electrochemical cycles, aging phenomena...), to nanomaterials for health and to understanding of corrosion process of various materials. He is a specialist of surface materials (XPS-AES,TOF-SIMS, AFM-STM), theoretical calculations.

Nicolas Louvain is Associate Professor at the University of Montpellier, working on Li-ion materials modification and advanced *operando* characterization techniques at the Institute Charles Gerhardt (ICGM). He developed the atomic layer fluorination method, an innovative way of using F atom and surface chemical bonding to improve the electrode reactivity during cycling.

Laure Monconduit is Research Director at the CNRS at the ICGM, in Montpellier. She has headed the "Batteries" research group since 2011. Her research focuses on the synthesis and characterization of new electrode materials for Li-ion and post-Li (Na, K, Mg, Ca-ion) with particular attention focused on the redox mechanisms of electrode materials and those occuring at the electrode/electrolyte interface, by operando techniques (DRX, Mössbauer, IR-ATR, Raman, XAS).

SUPPORTING INFORMATION

Additional supporting information may be found in the online version of the article at the publisher's website.

How to cite this article: Roland A, Fullenwarth J, Ledeuil J-B, Martinez H, Louvain N, Monconduit L. How carbon coating or continuous carbon pitch matrix influence the silicon electrode/electrolyte interfaces and the performance in Li-ion batteries. *Battery Energy*. 2022;1:20210009.
doi:10.1002/BTE2.20210009